Electronic Supplementary Material (ESI) for Journal of Materials Chemistry A.

Supporting Information

Modulating Electronic Structure of Triazine-based Covalent Organic Frameworks for Photocatalytic Organic Transformations

Zhangjie Gu, Jinjian Wang, Zhen Shan, Miaomiao Wu, Tongtong Liu, Liang Song, Guixiang Wang, Xuehai Ju, Jian Su,* and Gen Zhang*

Key Laboratory for Soft Chemistry and Functional Materials of Ministry of Education, School of Chemical Engineering, Nanjing University of Science and Technology, Nanjing, Jiangsu 210094, China.

Table of Content

S1. Materials and measurements

Materials.

All the chemicals are commercially available and used without further purification. 1,3,5-tris (4-aminophenyl) benzene (TAPB), 1,3,5-tri(4-formylphenyl) benzene (TFP), and tris(4-Aminophenyl) amine (TPA) energy chemical (Shanghai, China). Nafion mixture was purchased from Integrity technology (Shanghai, China). FTO Conductive glass was purchased from South China Xiang Cheng Technology (Yi yang, China), n-BuLi was purchased from j&k.

Measurements.

nuclear magnetic resonance (NMR): Liquid state ^{1}H ^{13}C NMR spectra of all the samples were collected on a Bruker Advance III instrument with AS500 magnet equipped with a cryoprobe (300 MHz).

Fourier transform infrared (FT-IR): Fourier transform infrared (FT-IR) spectra in the range of 4000 to 500 cm-1 were collected by Universal ATR accessory.

X-ray photoelectron spectroscopy (XPS): X-ray photoelectron spectroscopy (XPS) spectra were obtained by the Kratos axis supraTM of Shimadzu.

PXRD: PXRD patterns were collected on a Bruker D8 Advance diffractometer operated at 40 kV and 40 mA using Cu Kα radiation and in the range of 2-30°, the structure of COFs was simulated by Material Studio Software.

Scanning electron microscope (SEM): SEM images were collected using a Helios G4 CX.

Transmission electron microscope (TEM): TEM images were collected using a JEM-2800.

Gas adsorption: N_2 adsorption and desorption of COFs were performed at 77 K using ASAP 2020, Micromeritics Instrument Corp, USA. Pore size distributions and pore volumes were derived from the adsorption isotherms.

Thermogravimetric analysis (TGA): Thermogravimetric analysis (TGA) was carried out on the DTG-60AH from 30 to 800 °C under N_2 with a heating rate of 10 °C min^{-1}.

UV-Vis spectroscopy (UV-vis): The ultraviolet−visible diffuse reflectance spectroscopy (UV−vis DRS) was conducted on Shimadzu UV-2600 tested from 220 to 800 nm.

The time-resolved photoluminescence (TRPL): The time-resolved photoluminescence (TRPL) was carried on Edinburgh, UK FS5.

The electron paramagnetic (EPR) measurements: 10mg COFs powder was dispersed in 10ml solvent, after dispersion, taking 200 μl of sample solution and adding 10 μl of DMPO or TEMPO, mix well and load the sample for test on Bruker A300/E500 at room temperature with light irradiation using a 300 W Xe lamp.

Photoelectrochemical measurements: Photoelectrochemical measurements were performed on an electrochemical workstation (CHI 660E, CH Instruments Inc., Shanghai). The preparation method of the working electrode is as follows: First, weigh 5 mg of COFs and put it into the quartz glass vial, adding 1ml ethanol and 30 μl Nafion mixture solution, subsequently, ultrasound for 60 minutes. Then, 100 μl mixture was transferred into the FTO with 1 × 1 cm^2 illuminated area and dried at 80℃ for 8 h. Platinum electrode as the auxiliary electrode, Ag/AgCl electrode as reference electrode, Na_2SO_4 (0.2 M) solution was used as the electrolyte solution. Mott−Schottky (M−S) plots were recorded from -1.2 V to 1.2 V at a scan rate of 5 mV/s in the dark at frequencies of 1000 Hz. Liner sweep voltammetry (LSV) curves were recorded at a scan rate of 0.01 V/s from−0.8 to 0.3 V in the light. The on−off transient photocurrent responses were recorded with a sampling interval of 20 s using a 300 W (100 Mw/cm^2) Xe lamp with a 400 nm-cut filter lamp and a certain applied bias of 0 V. Electrochemical impedance spectroscopy measurements were recorded 10 mV amplitude with over a 0.01 to 10^6 Hz frequency range.

S2. Experimental procedures

Synthesis of 5-Bromothiophene-2-carbonitrile.

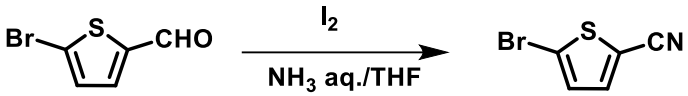

5-bromothiophene-2-carboxaldehyde (10 g, 52.5 mmol) was dissolved in THF (35 ml), and aqueous ammonia (ca. 28 %, 105 mL). Then iodine was added slowly (15 g, 57.6 mmol), The reaction mixture was stirred for 12 h at room temperature, and then quenched with an aqueous $Na_2S_2O_3$ (ca. 5%, 40 mL). The product was extracted with DCM. The organic layer wash with water for many times and dried over anhydrous $MgSO_4$. the residue was purified by silica gel column chromatography (eluent: DCM/hexane = 3:1, v/v), and dried under vacuum to yield 5-Bromothiophene-2-carbonitrile as a light-yellow oil (yield = 8.9 g, 90%).

Synthesis of 2,4,6-Tris(5-bromothiophene-2-yl)-1,3,5-triazine.

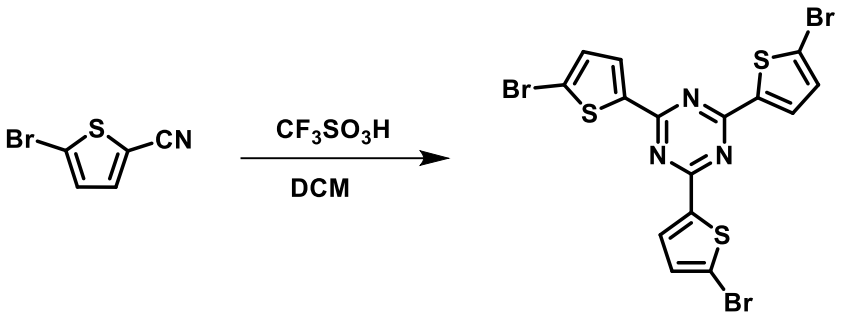

TBPT

To a stirred solution of 5-Bromothiophene-2-carbonitrile (3.17 g, 16.86 mmol) in dry CH_2Cl_2 (80 mL), then trifluoromethanesulfonic acid (2.53 g, 16.86 mmol) was added at 0 °C. The mixture was stirred for 36 h at room temperature. After the solvent was removed, the residue was neutralized with an aqueous $NaHCO_3$. The formed precipitate was collected by filtration, washed with water, methanol, acetone, and hexane in this order, and then dried under vacuum to afford 2 as an off-white solid (yield = 2.6 g, 82 %).

Synthesis of 5,5',5''-(1,3,5-triazine-2,4,6-triyl) tris(thiophene-2-carbaldehyde) (3TT).

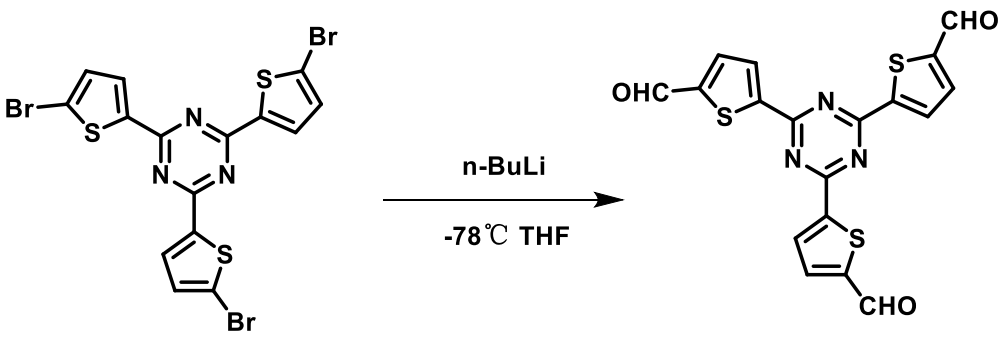

3TT

2,4,6-Tris(5-bromothiophene-2-yl)-1,3,5-triazine (0.6 g 1.06 mmol) was dissolved in dry THF (120 ml) and keep temperature at -78 ℃.Then n-BuLi (1.68 mL, 2.4 M in hexane) was added dropwise ,after 2 h at -78 ℃， the dry DMF was added dropwise, and then the reaction mixture was warmed up slowly to ambient temperature overnight. The reaction was quenched with water. Subsequently, the solvent was removed and extracted with DCM. The residue was purified by silica gel column chromatography (eluent: DCM) to give a yellow solid (yield = 98 mg, 22 %). ^{1}H NMR (500 MHz, $CDCl_3$): δ 10.04 (s,3H). 8.36-8.35 (d, 3H). 7.88-7.87 (d, 3H).

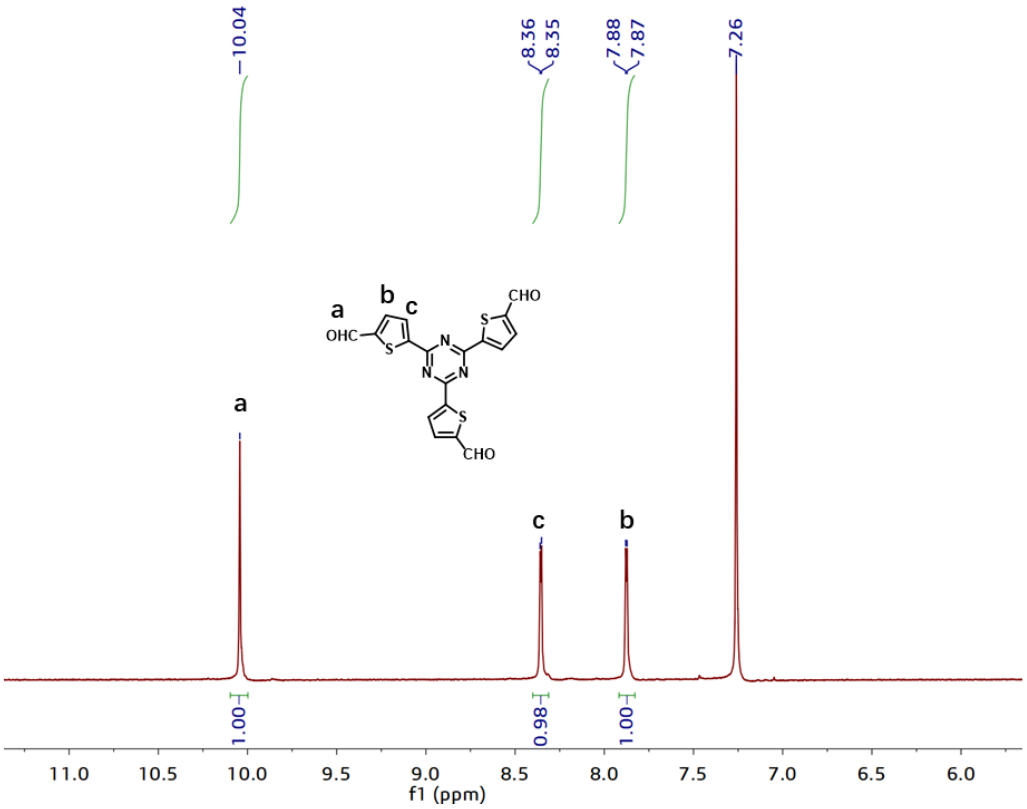

Figure S1. ^{1}H NMR spectrum of 3TT.

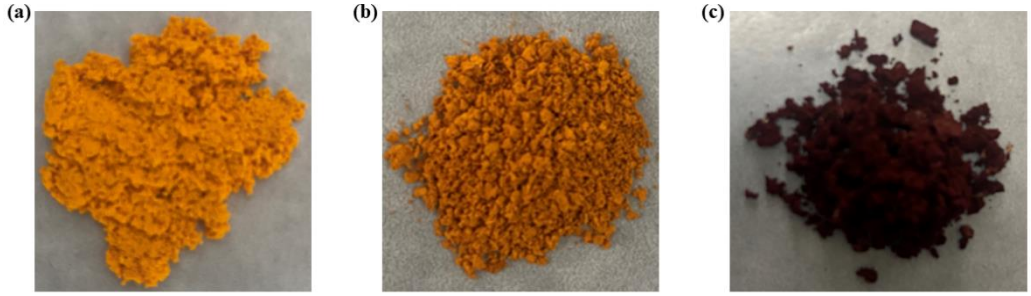

Figure S2. The photo of COFs. (a) COF-NUST-31, (b) COF-NUST-32, (c) COF-NUST-33.

S3. Supplementary characterization.

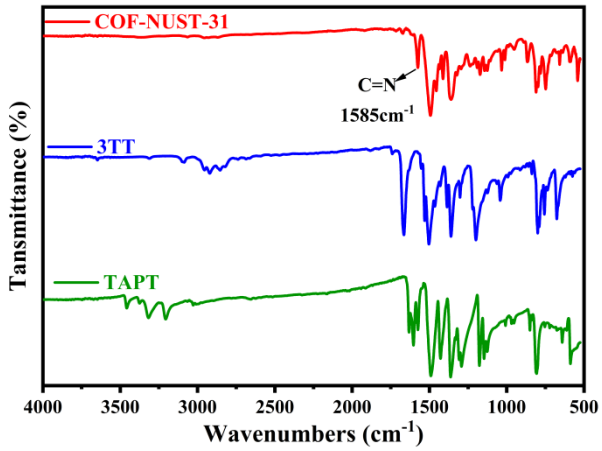

Figure S3. FTIR spectra of COF-NUST-31, 3TT, and TAPT.

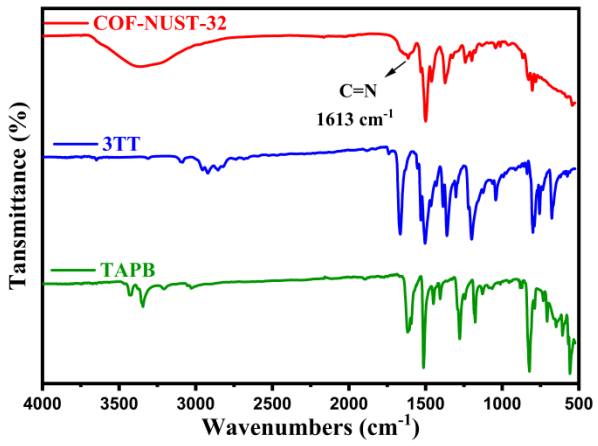

Figure S4. FTIR spectra of COF-NUST-32, 3TT, and TAPB.

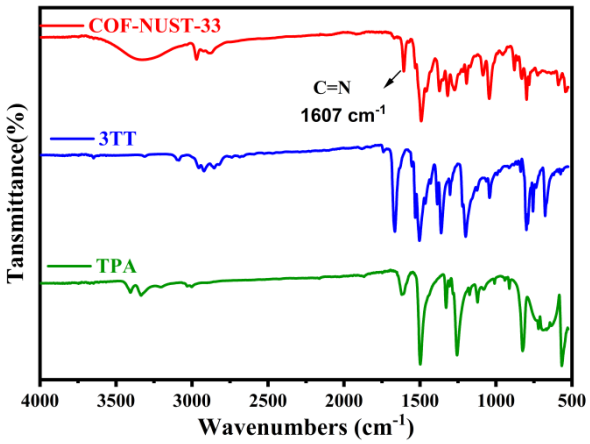

Figure S5. FTIR spectra of COF-NUST-33, 3TT, and TPA.

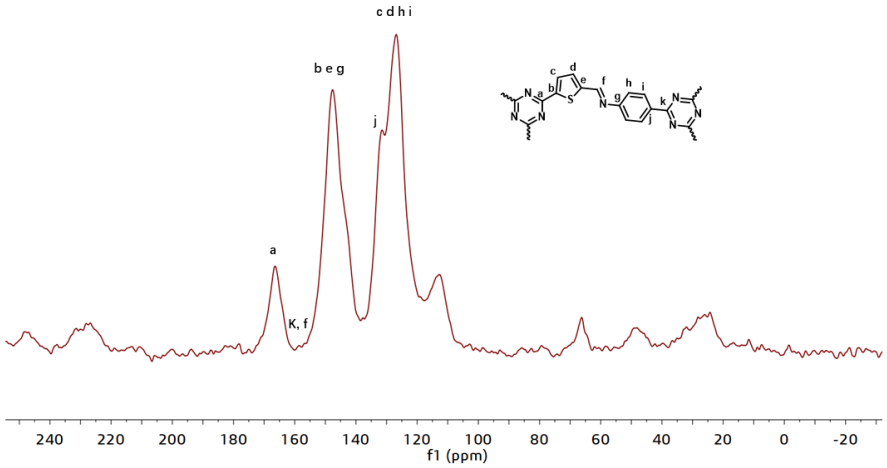

Figure S6. ^{13}C-NMR spectrum of COF-NUST-31.

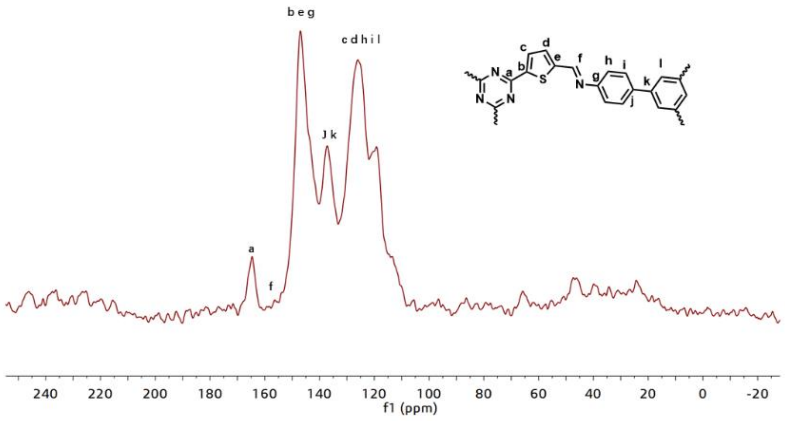

Figure S7. ^{13}C-NMR spectrum of COF-NUST-32.

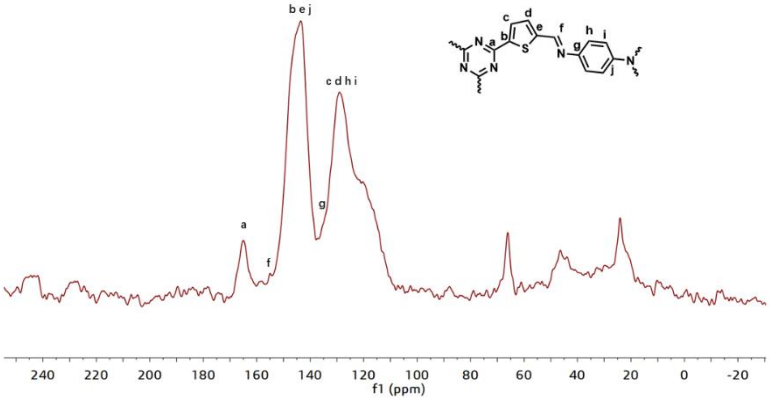

Figure S8. ^{13}C-NMR spectrum of COF-NUST-33.

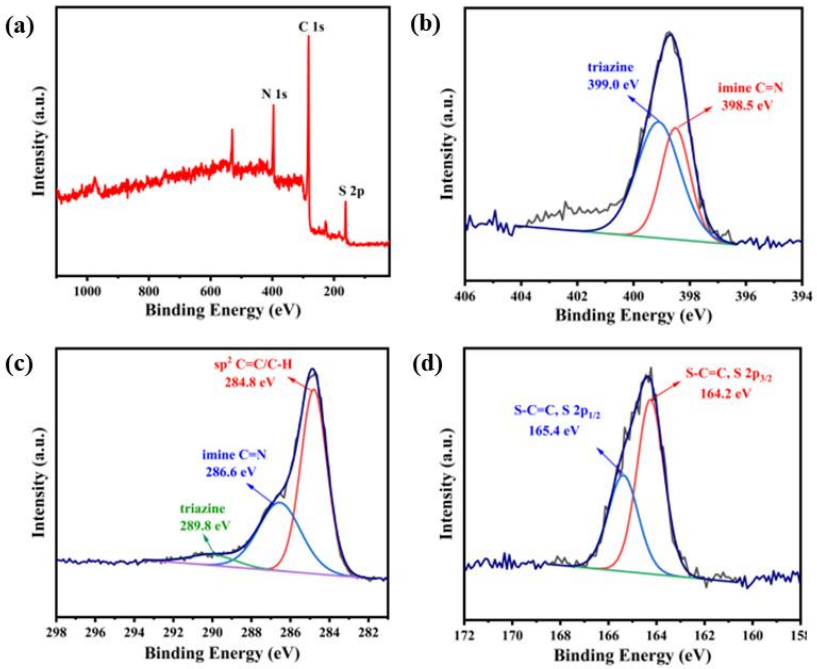

Figure S9. XPS spectra of COF-NUST-31. (a) Survey, (b) N 1s, (c) C 1s, and (d) S 2p.

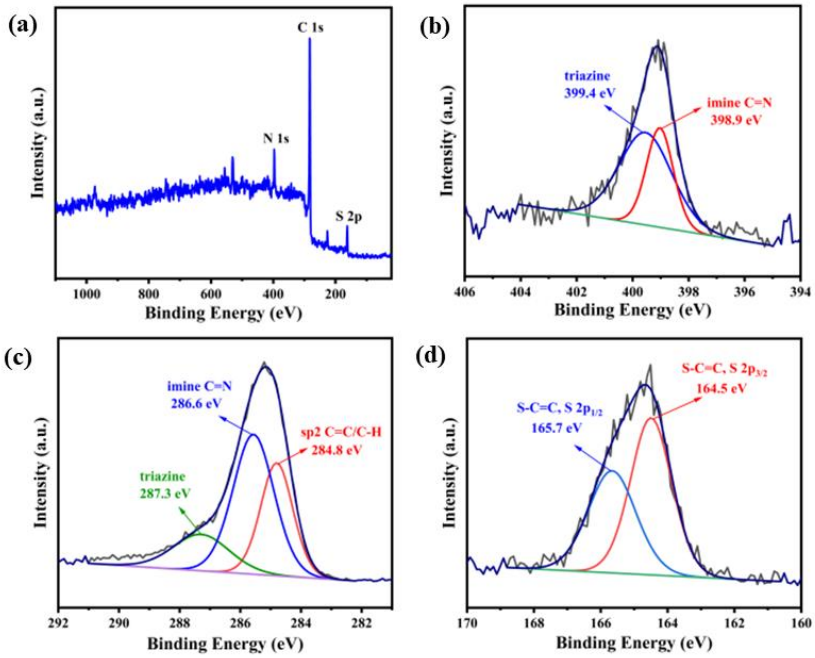

Figure S10. XPS spectra of COF-NUST-32. (a) Survey, (b) N 1s, (c) C 1s, and (d) S 2p.

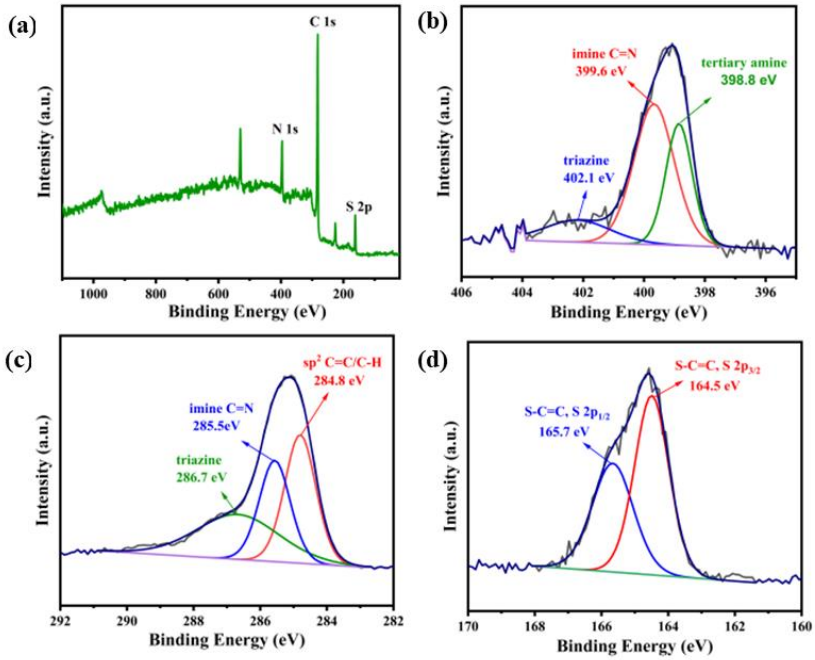

Figure S11. XPS spectra of COF-NUST-33. (a) Survey, (b) N 1s, (c) C 1s, and (d) S 2p.

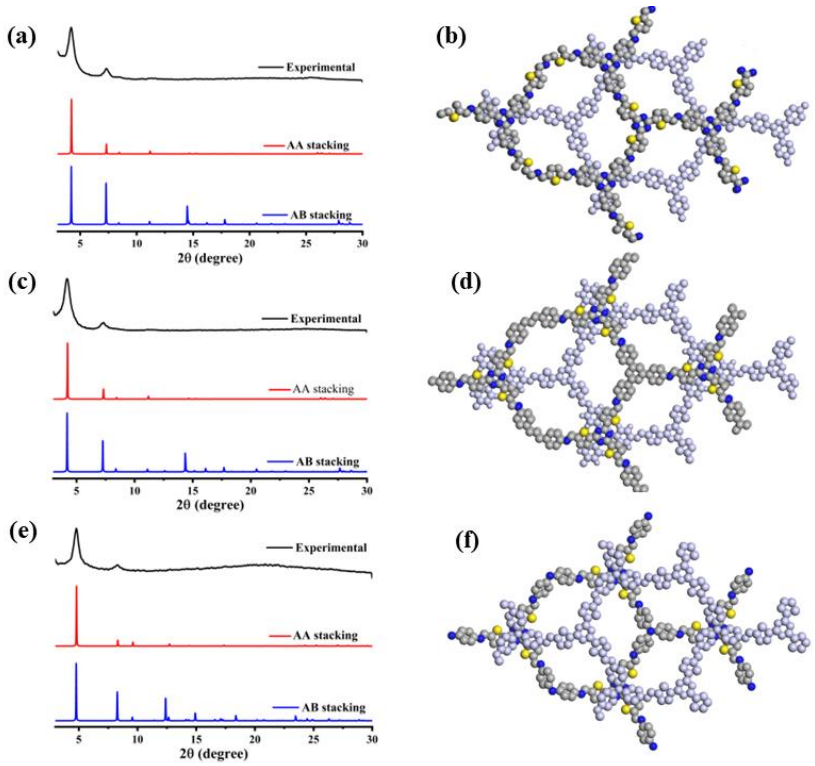

Figure S12. Simulated PXRD patterns and top views for AB stacking of COF-NUST-31 (a) (b), COF-NUST-32 (c) (d), and COF-NUST-33 (e) (f).

Table S1. Fractional atomic coordinates for simulated COF-NUST-31.

Space group: *P3*			
3D hexagonal; a = b = 24.34 Å, c = 3.43 Å; α = β = 90°, γ = 120°			
Atom	x	y	z
N1	-0.28857	-0.68586	1.21966
C2	-0.26872	-0.62332	1.22007
C3	-0.20175	-0.57769	1.16204
C4	-0.17832	-0.51361	1.11677
C5	-0.11543	-0.48283	1.02536
C6	-0.09275	-0.52438	1.00263
S7	-0.14719	-0.60124	1.09829
C8	-0.02854	-0.50666	0.88762
N9	0.00971	-0.4505	0.75496
C10	0.073	-0.42889	0.62491
C11	0.11404	-0.3638	0.58913
C12	0.17722	-0.34036	0.48822
C13	0.20006	-0.38206	0.41766
C14	0.15799	-0.44748	0.43308
C15	0.09497	-0.47079	0.5334
C16	0.26803	-0.35764	0.35605
N17	0.291	-0.39784	0.35614
H18	-0.20612	-0.49044	1.13962
H19	-0.08775	-0.43254	0.96992
H20	-0.01434	-0.54186	0.91639
H21	0.09745	-0.3311	0.65217
H22	0.20839	-0.28964	0.47626
H23	0.17387	-0.48084	0.37333
H24	0.06415	-0.52146	0.53834

Table S2. Fractional atomic coordinates for simulated COF-NUST-32.

Space group: *P3*			
3D hexagonal; a = b = 24.28 Å, c = 3.42 Å; α = β = 90°, γ = 120°			
Atom	x	y	z
C1	-0.27168	-0.61945	0.05478
N2	-0.31887	-0.60515	0.05636
C3	-0.20583	-0.56954	0.11147
C4	-0.1866	-0.50578	0.15198
C5	-0.12368	-0.47111	0.25148
C6	-0.09738	-0.5098	0.28644
S7	-0.14768	-0.5881	0.19053
C8	-0.03271	-0.48892	0.41071
N9	0.00622	-0.43031	0.50673
C10	0.07041	-0.40863	0.62543
C11	0.11677	-0.34588	0.54753
C12	0.181	-0.32618	0.60125
C13	0.19992	-0.36842	0.75313
C14	0.15202	-0.42971	0.86514
C15	0.08847	-0.45007	0.79262
C16	0.26845	-0.35027	0.77926
C17	0.28624	-0.39721	0.78137
H18	-0.21738	-0.48567	0.12095
H19	-0.0987	-0.42037	0.30565
H20	-0.01791	-0.52421	0.41063
H21	0.10344	-0.31352	0.41795
H22	0.21496	-0.27904	0.50051
H23	0.16266	-0.46274	1.01081
H24	0.0537	-0.49823	0.87261
H25	0.25012	-0.44651	0.77663

Table S3. Fractional atomic coordinates for simulated COF-NUST-33.

Space group: *P3*			
3D hexagonal; a = b = 21.32 Å, c = 4.05 Å; α = β = 90°, γ = 120°			
Atom	x	y	z
C1	0.73804	0.38519	0.50336
N2	0.68611	0.40437	0.50145
C3	0.81323	0.43952	0.42626
C4	0.83777	0.51301	0.40127
C5	0.90531	0.54938	0.26004
C6	0.93007	0.50246	0.17895
S7	0.87285	0.41409	0.28264
C8	0.99861	0.52363	0.01171
N9	0.04384	0.59103	-0.05877
C10	0.11437	0.61498	-0.19581
C11	0.17139	0.68231	-0.09819
C12	0.24287	0.70086	-0.16646
C13	0.25911	0.65357	-0.34468
C14	0.20042	0.5899	-0.47566
C15	0.12907	0.56985	-0.39621
H18	0.80667	0.53864	0.47035
H19	0.93421	0.60716	0.21033
H20	1.01281	0.48192	-0.02947
H21	0.16083	0.71798	0.05438
H22	0.28484	0.75115	-0.06686
H23	0.20943	0.55216	-0.61522
H24	0.08587	0.51794	-0.48244
N	0.33333	1.66667	0.63226

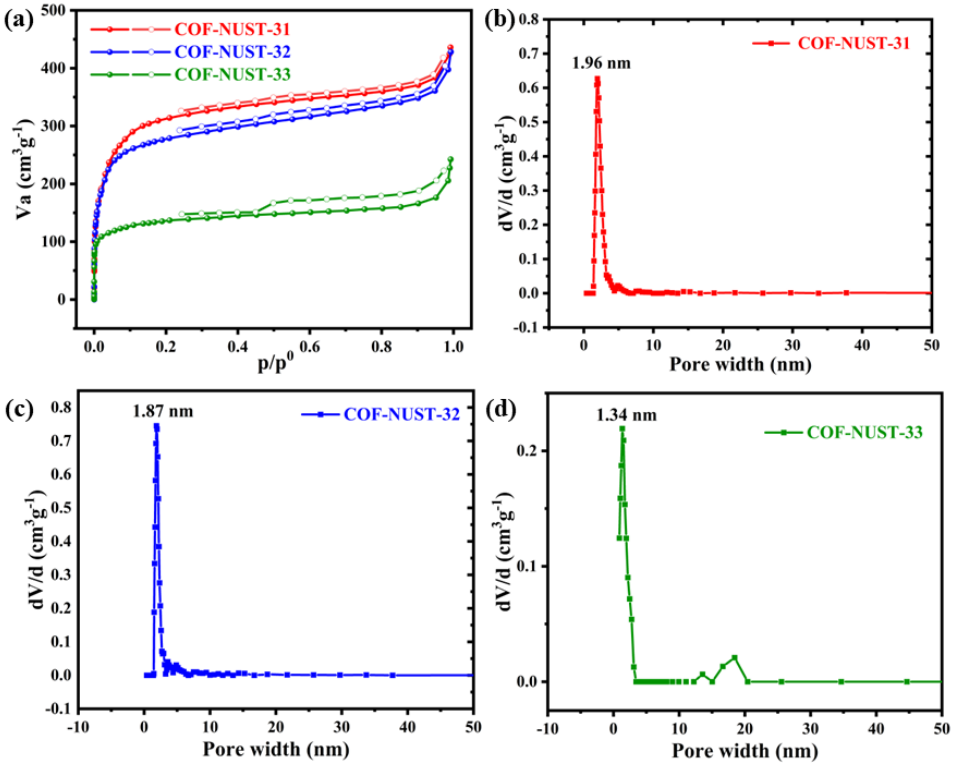

Figure S13. (a) N_2 adsorption-desorption isotherms at 77 K of COFs powders. Pore size distribution of COF-NUST-31 (b), COF-NUST-32 (c), and COF-NUST-33 (d).

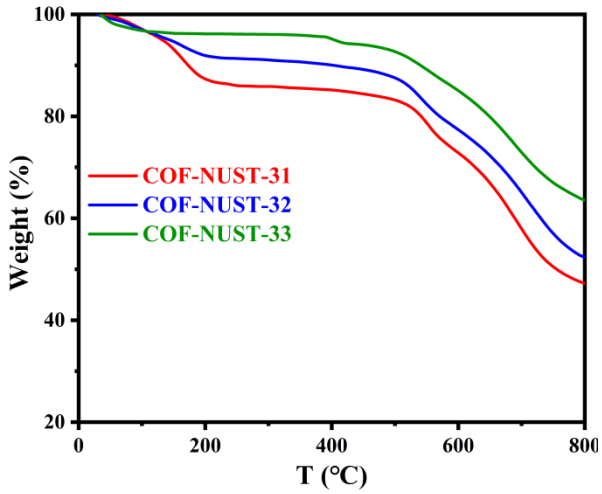

Figure S14. TGA curves of COFs.

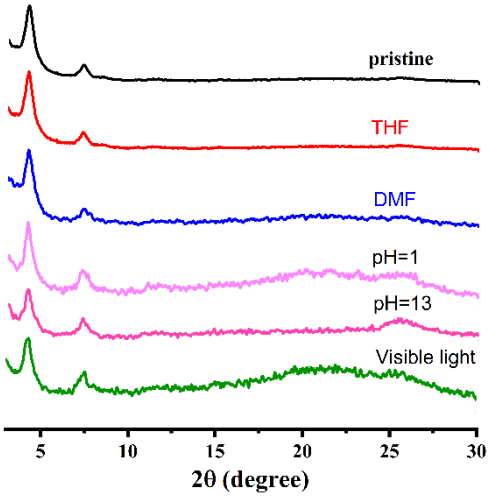

Figure S15. PXRD patterns at different conditions for COF-NUST-31.

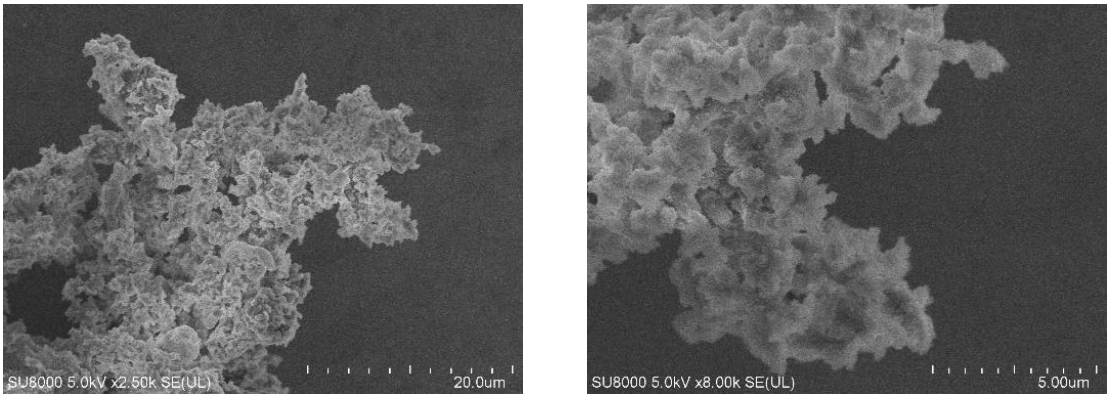

Figure S16. Scanning electron microscopy (SEM) images of COF-NUST-31.

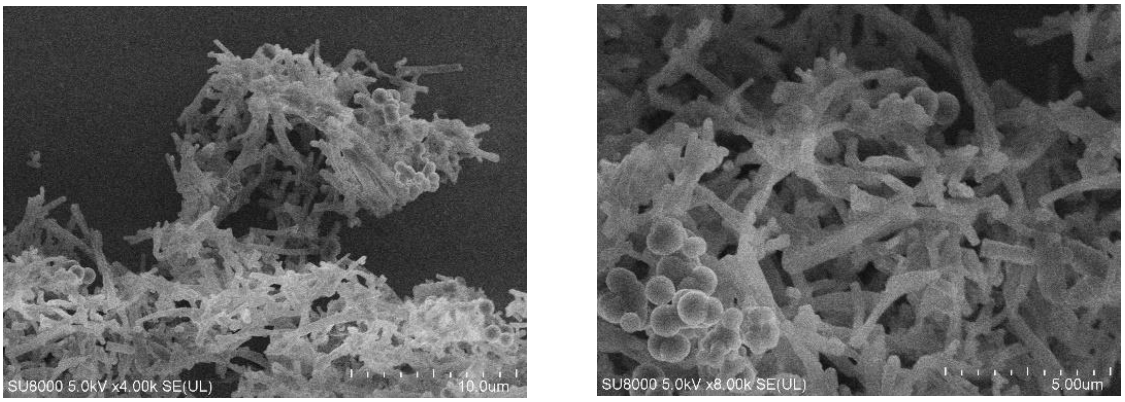

Figure S17. Scanning electron microscopy (SEM) images of COF-NUST-32.

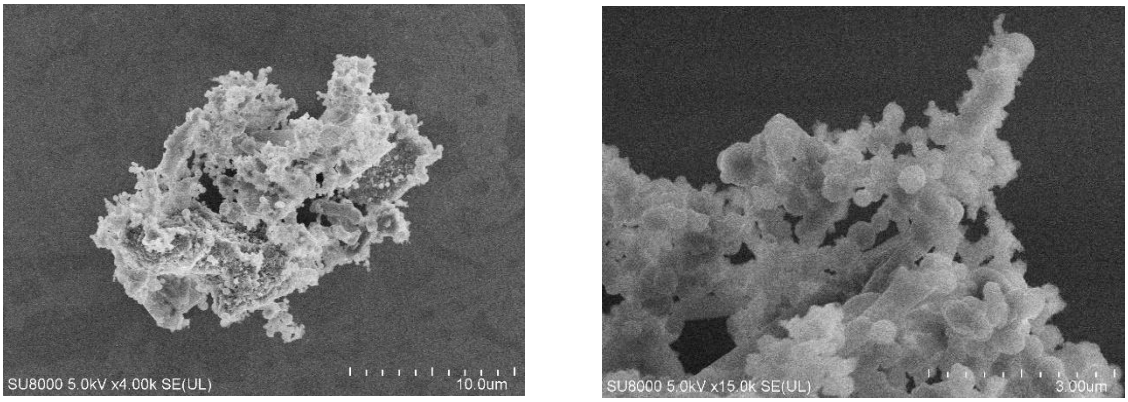

Figure S18. Scanning electron microscopy (SEM) images of COF-NUST-33.

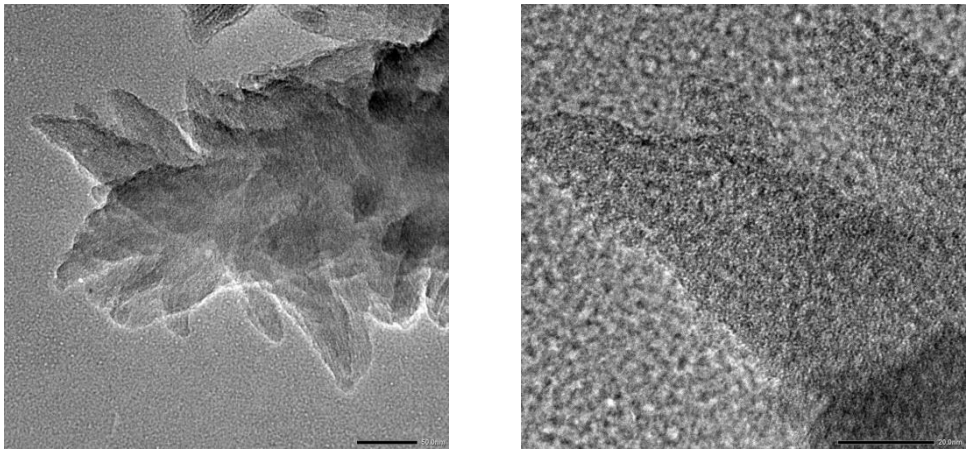

Figure S19. Transmission electron microscopy (TEM) images of COF-NUST-31.

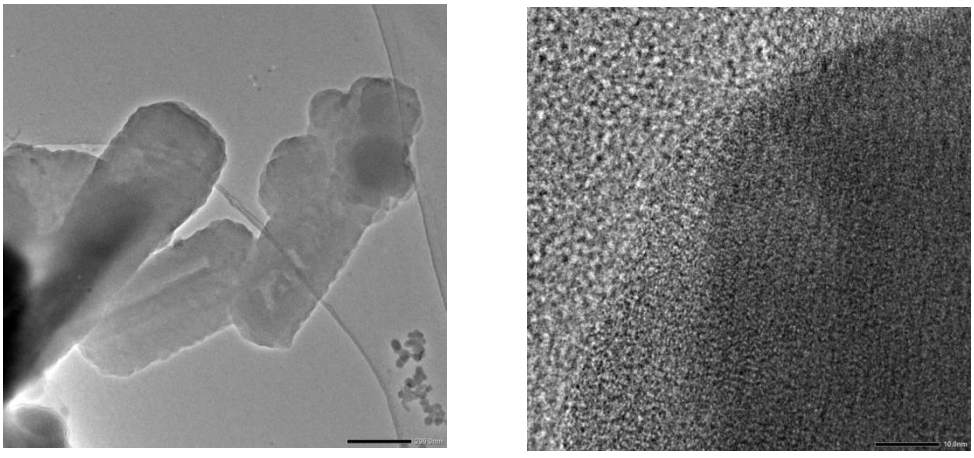

Figure S20. Transmission electron microscopy (TEM) images of COF-NUST-32.

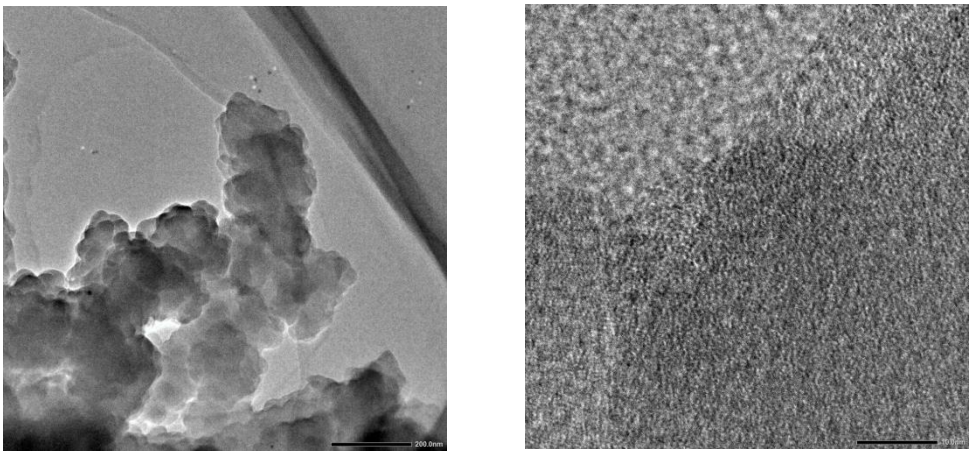

Figure S21. Transmission electron microscopy (TEM) images of COF-NUST-33.

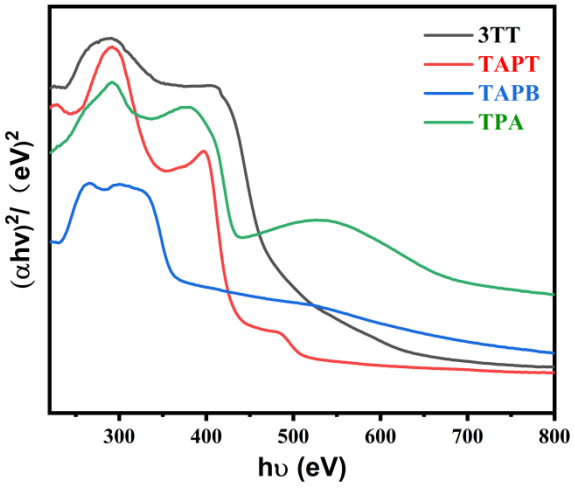

Figure S22. The UV−vis diffuse reflectance spectroscopy of monomers.

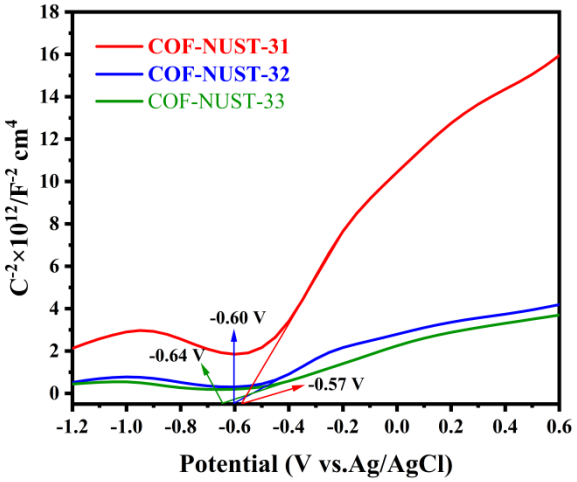

Figure S23. Mott-Schottky plots of COFs at frequencies of 1000 Hz.

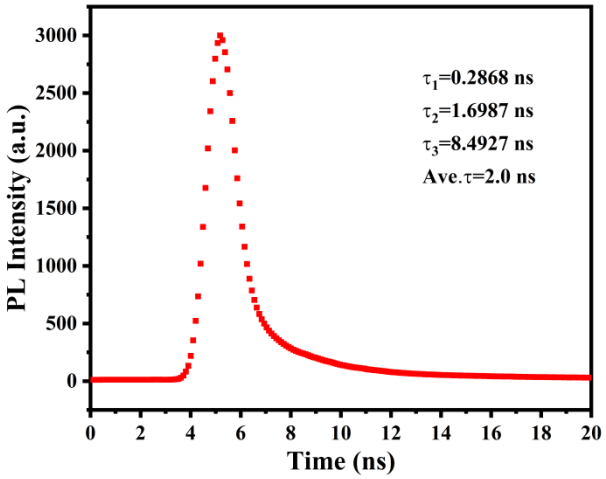

Figure S24. TRPL spectrum for COF-NUST-31.

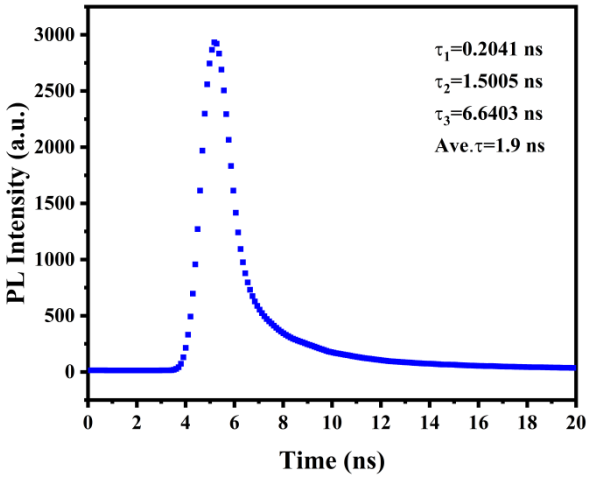

Figure S25. TRPL spectrum for COF-NUST-32.

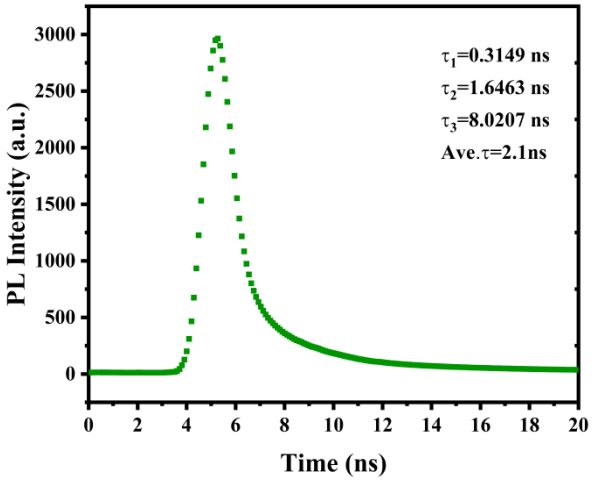

Figure S26. TRPL spectrum for COF-NUST-33.

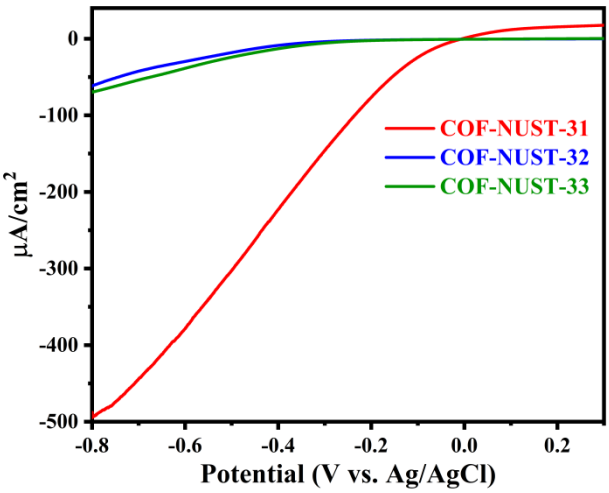

Figure S27. LSV curves under visible light irradiation.

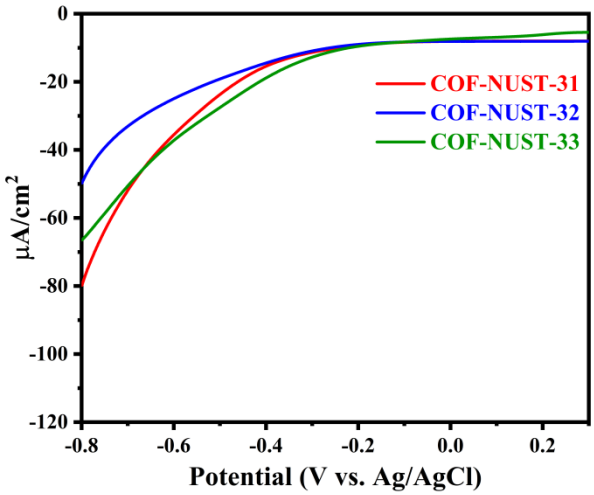

Figure S28. LSV curves under dark.

Table S4. The calculated HOMO-LUMO gaps of COFs (in eV)

	COF-NUST-31	COF-NUST-32	COF-NUST-33
HOMO	-2.44	-1.85	-1.47
LUMO	-0.42	-0.17	-0.34
Band gap	2.01	1.68	1.13

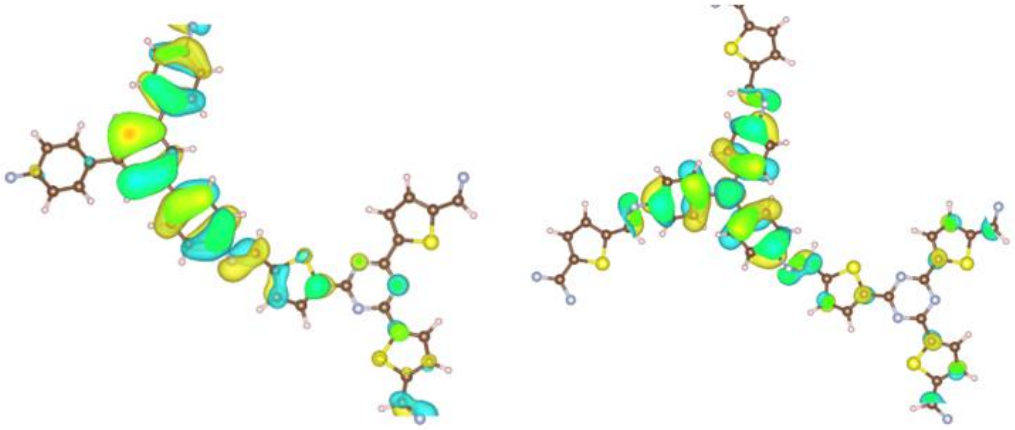

COF-NUST-32 COF-NUST-33

Figure S29. HOMO of COF-NUST-32 and COF-NUST-33.

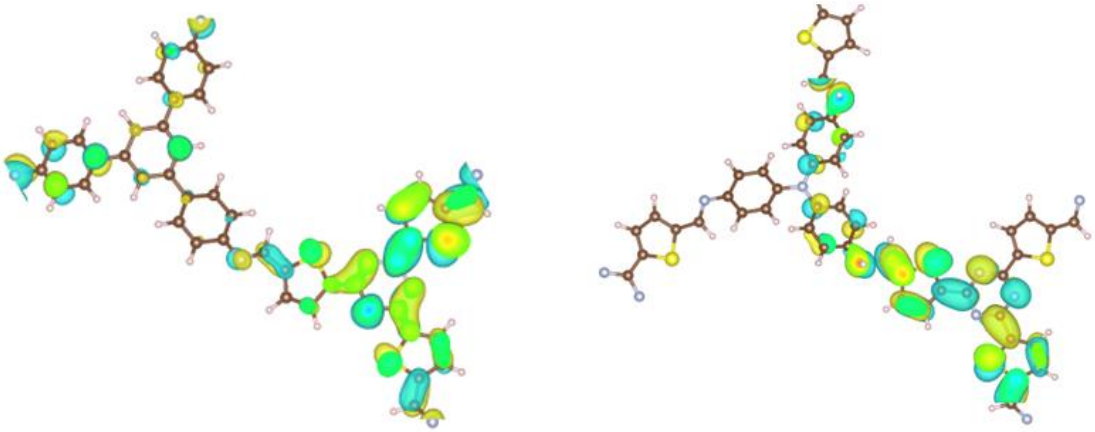

COF-NUST-32 COF-NUST-33

Figure S30. LUMO of COF-NUST-32 and COF-NUST-33.

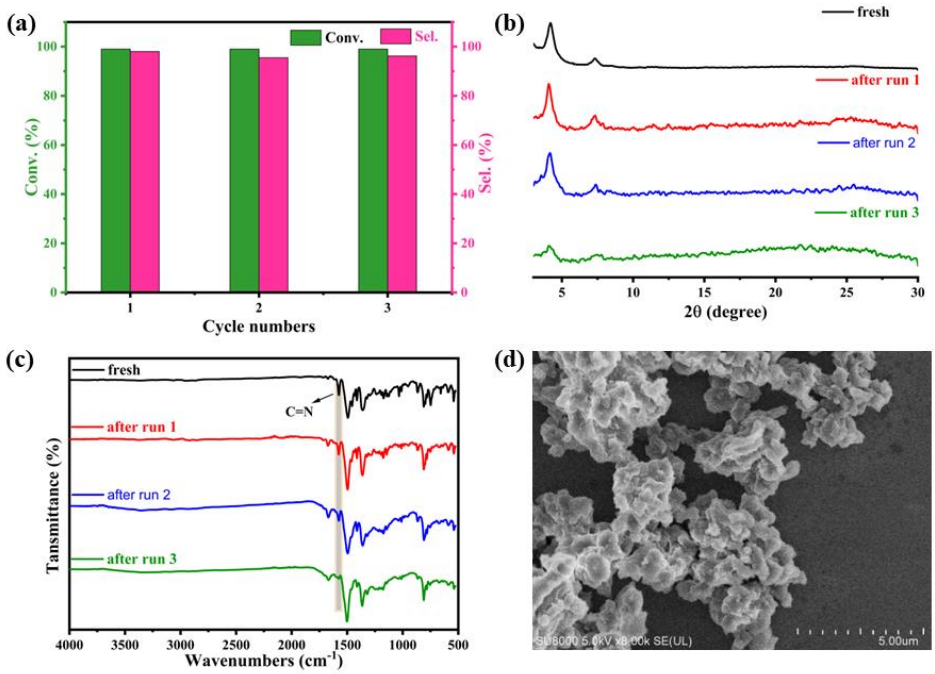

Figure S31. (a) The recycling ability of COF-NUST-31 in selective aerobic oxidation of sulfide. (b) PXRD of recovered COF-NUST-31. (c) Fourier transform infrared (FTIR) spectra of recovered COF-NUST-31. (d) Scanning electron microscopy (SEM) images of recovered COF-NUST-31.

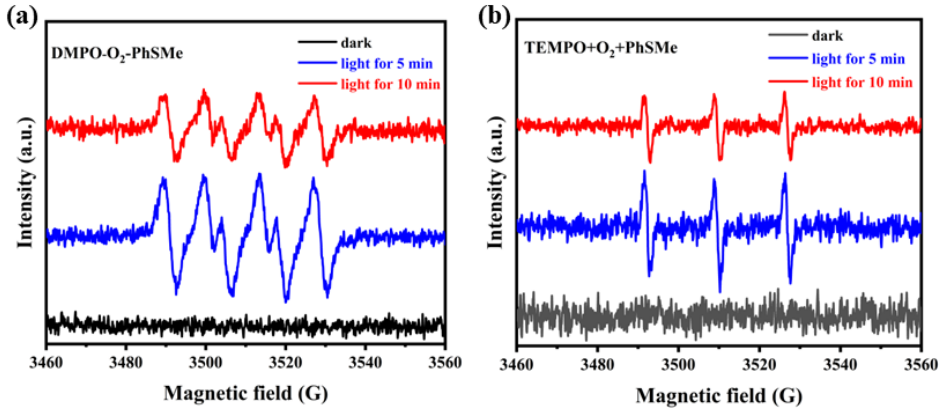

Figure S32. $^{\bullet}O_2^-$ and $^1O_2$ signal attenuation after adding PhSMe under elongated light illumination.

Table S5. Photocatalytic performances in this work compared with previous results based on inorganic or organic materials in the literatures.

Catalyst	Catalyst weight (mg)	Substrate Amount (mmol)	O_2 Pressue (atm)	Light source	Time (h)	Yield (%)	Reference
ARS-TiO_2	9.6 mg	0.3 mmol and 0.006 mmol TEMPO	1 atm O_2	300 W Xe lamp	3	84	[1]
polyimide-P25	25 mg	0.3 mmol and 0.036 mmol ETA	1atm air	12 W blue light	2	94	[2]
$Bi_4O_5Br_2$	20 mg	0.2 mmol	1 atm O_2	30 W blue light	6	99	[3]
TiO2	40 mg	0.3 mmol	1 atm O_2	300 W Xe lamp	5	58	[4]
Ti-MCM-48	25 mg	0.5 mmol and ARS (0.001 mmol)	1 atm air	12 W green light	1.1	91	[5]
CF-HCP	5 mg	0.2 mmol	1 atm O_2	100 W Green light	6	99	[6]
BBT@ TiO_2-0.8	5 mg	1 mmol	1 atm O_2	Blue light	20	99	[7]
AQ-COF	10 mg	0.1 mmol	1 atm O_2	300 W Xe lamp	3	99	[8]
COF-NUST-32	4 mg	0.1 mmol	1 atm O_2	30 W Blue light	4	98	This work

S4. Photocatalytic performances of ^{1}H-NMR spectra.

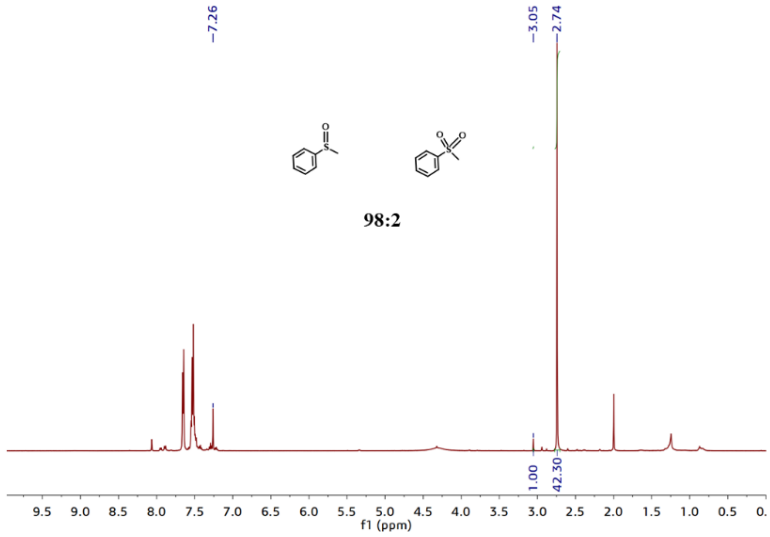

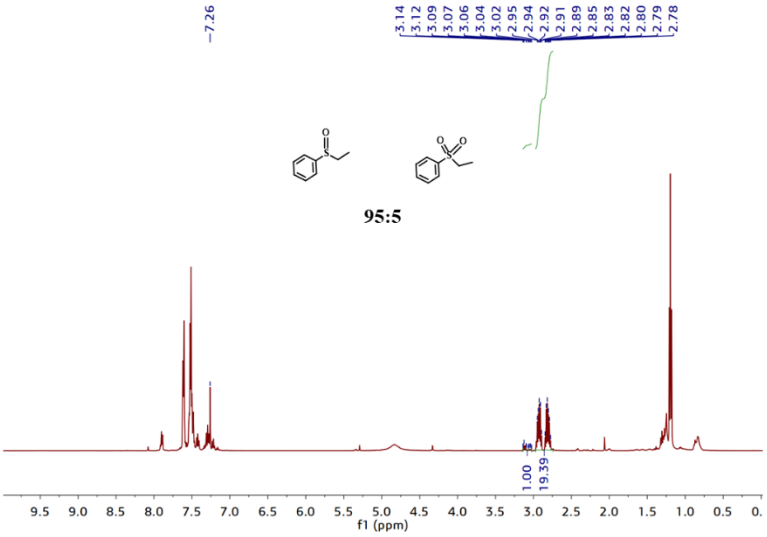

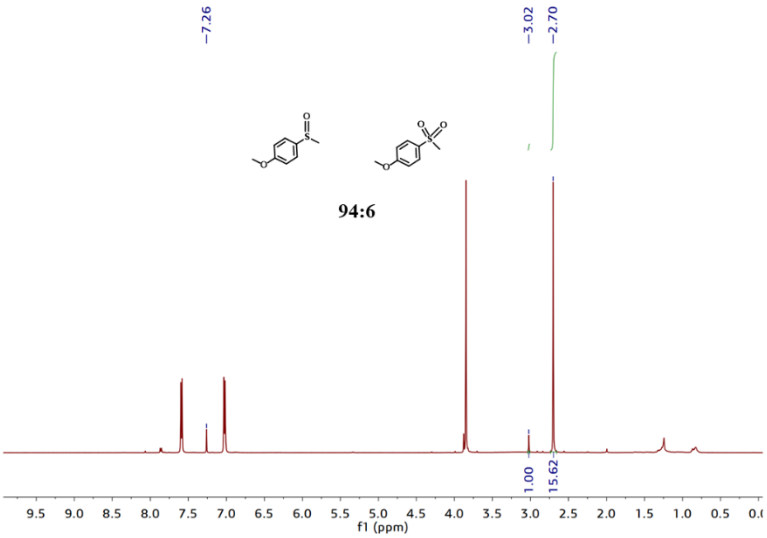

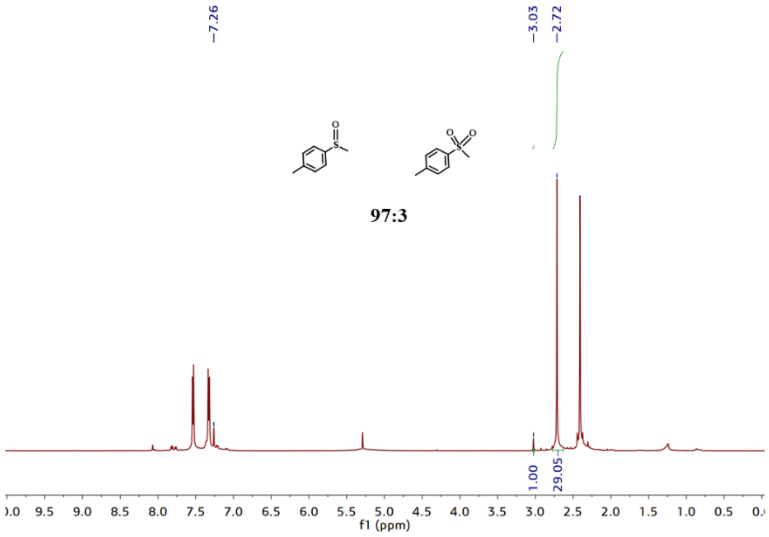
7.26
3.03
2.72
1.00
29.05
f1 (ppm)

97:3

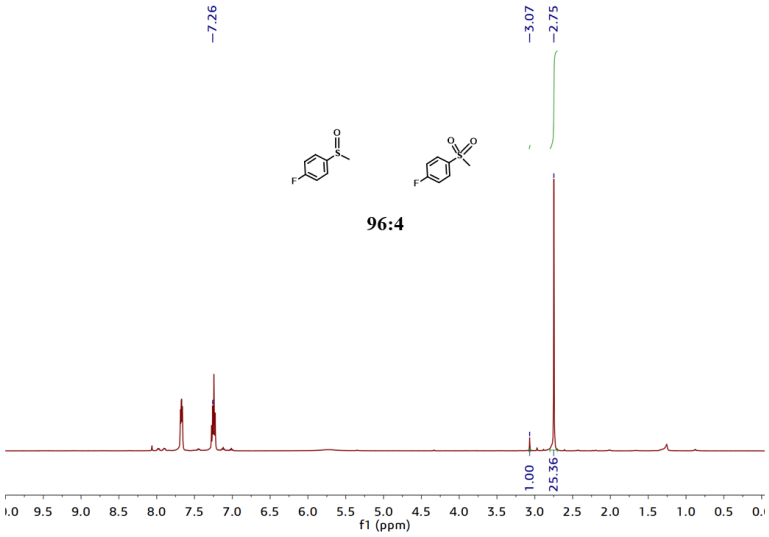
7.26
3.07
2.75
1.00
25.36
f1 (ppm)

96:4

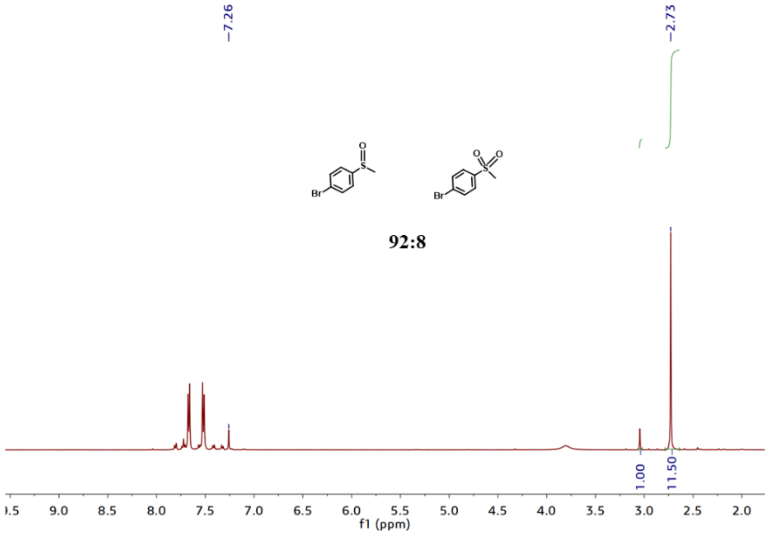
7.26
2.73
1.00
11.50
f1 (ppm)

92:8

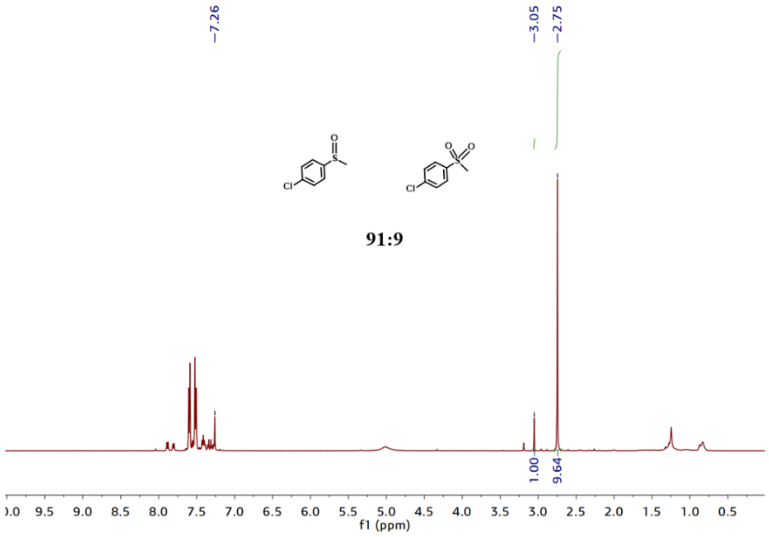
7.26
3.05
2.75
91:9
1.00
9.64
f1 (ppm)

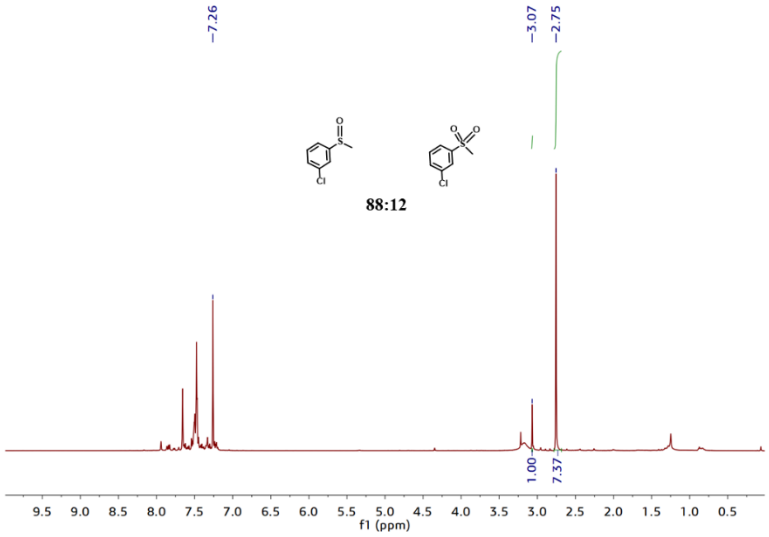
7.26
3.07
2.75
88:12
1.00
7.37
f1 (ppm)

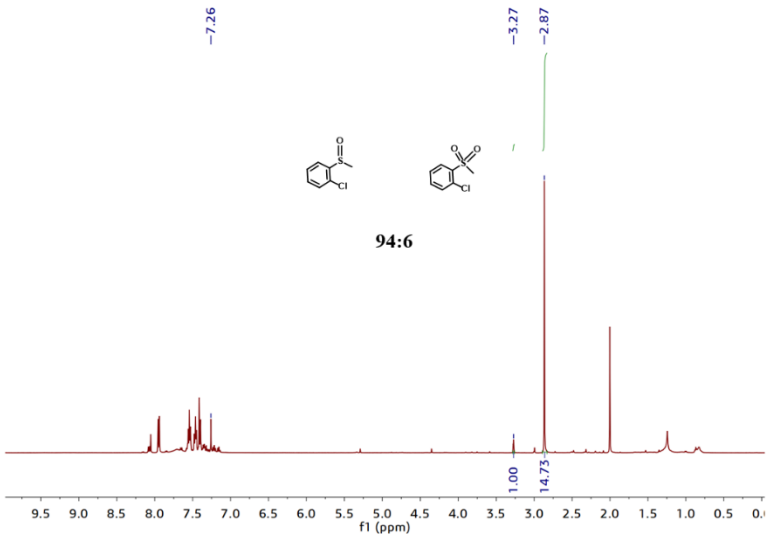
7.26
3.27
2.87
94:6
1.00
14.73
f1 (ppm)

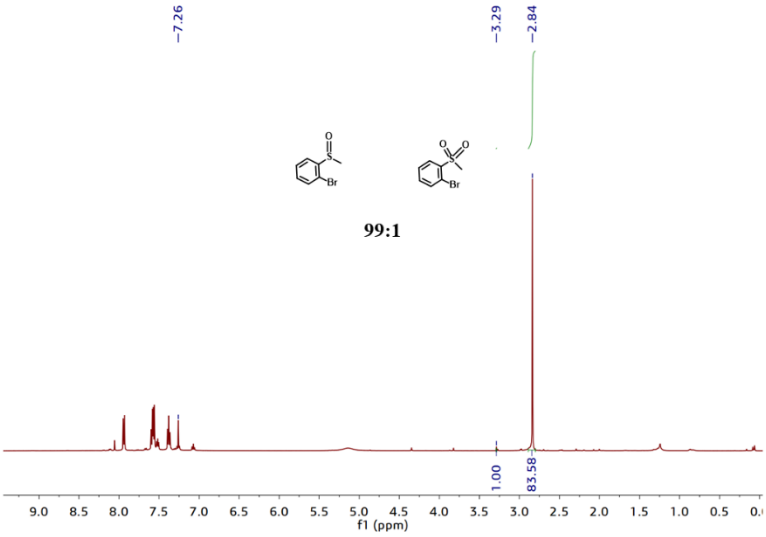
7.26
3.29
2.84
99:1
1.00
83.58
f1 (ppm)

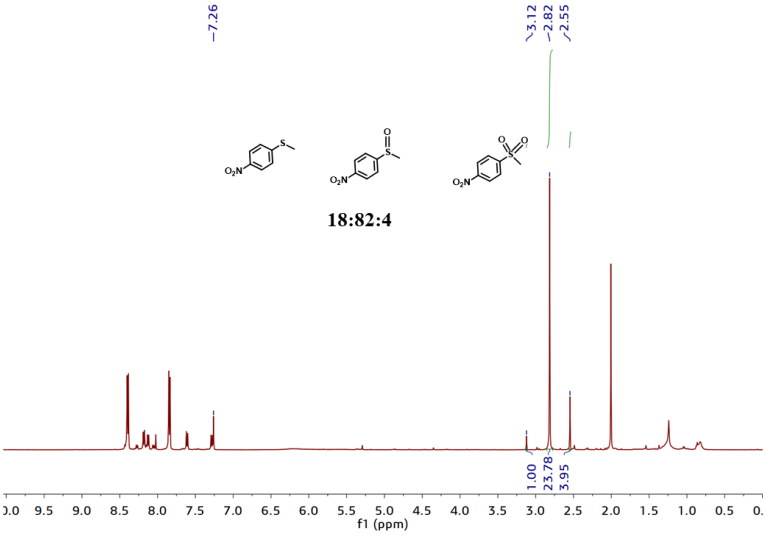
7.26
3.12
2.82
2.55
18:82:4
1.00
23.78
3.95
f1 (ppm)

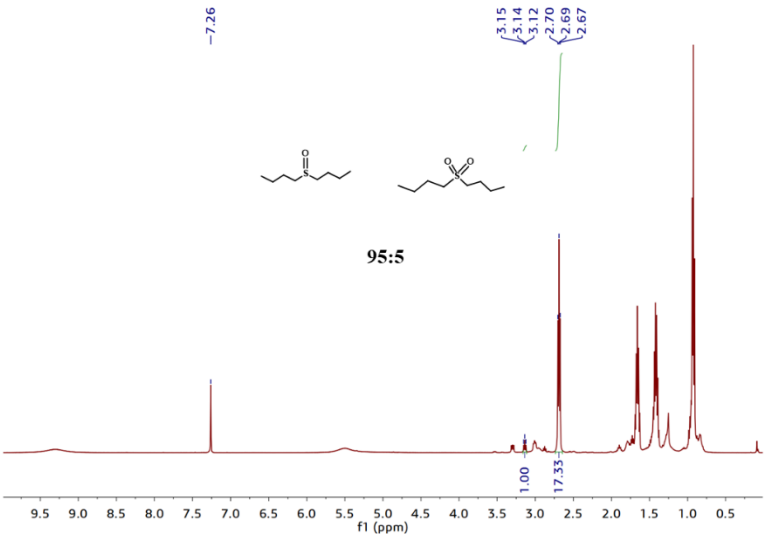
7.26
3.15
3.14
3.12
2.70
2.69
2.67
95:5
1.00
17.33
f1 (ppm)

S5. Reference

1. X. J. Lang, J. C. Zhao and X. D. Chen, *Angew. Chem. , Int. Ed.*, 2016, **55**, 4697-4700.
2. W. L. Sheng, J. L. Shi, H. M. Hao, X. Li and X. J. Lang, *J. Colloid Interf Sci.*, 2020, **565**, 614-622.
3. W. Zhao, C. X. Yang, J. D. Huang, X. L. Jin, Y. Deng, L. Wang, F. Y. Su, H. Q. Xie, P. K. Wong and L. Q. Ye, *Green Chem.*, 2020, **22**, 4884-4889.
4. X. J. Lang, W. Hao, W. R. Leow, S. Z. Li, J. C. Zhao and X. D. Chen, *Chem. Sci.*, 2015, **6**, 5000-5005.
5. F. W. Huang, H. M. Hao, W. L. Sheng, X. Y. Dong and X. J. Lang, *Chem. Eng. J.*, 2022, **432**, 134285.
6. Y. F. Zhi, K. Li, H. Xia, M. Xue, Y. Mu and X. M. Liu, *J. Mater. Chem. A.*, 2017, **5**, 8697-8704.
7. C. Ayed, W. Huang, R. Li, L. C. da Silva, D. Wang, O. Suraeva, W. Najjar and K. A. I. Zhang, *Part. Part. Syst. Charact.*, 2018, **35**, 1700234.
8. Q. Li, X. W. Lan, G. Y. An, L. Ricardez-Sandoval, Z. G. Wang and G. Y. Bai, *ACS. Catal.*, 2020, **10**, 6664-6675.